High Order Recurrent Neural Control for Wind Turbine with a Permanent Magnet Synchronous Generator

Control Neuronal Recurrente de Alto Orden para Turbinas de Viento con Generador Síncrono de Imán Permanente

Luis J. Ricalde[1], Braulio J. Cruz[1] and Edgar N. Sánchez[3]

[1]UADY, Facultad de Ingeniería, Av. Industrias no Contaminantes por Periférico Norte Apdo. Postal 115 Cordemex, Mérida, Yucatán, México
lricalde@uady.mx
[2]CINVESTAV, Unidad Guadalajara, Apartado Postal 31-430, Plaza La Luna, C.P. 45091, Guadalajara, Jalisco México
sanchez@gdl.cinvestav.mx

Article received March 18, 2009; accepted on 23 September, 2009

Abstract. In this paper, an adaptive recurrent neural control scheme is applied to a wind turbine with permanent magnet synchronous generator. Due to the variable behavior of wind currents, the angular speed of the generator is required at a given value in order to extract the maximum available power. In order to develop this control structure, a high order recurrent neural network is used to model the turbine-generator model which is assumed as an unknown system; a learning law is obtained using the Lyapunov methodology. Then a control law, which stabilizes the reference tracking error dynamics, is developed using Control Lyapunov Functions. Via simulations, the control scheme is applied to maximum power operating point on a small wind turbine.

Keywords: Neural networks, Wind turbine, Permanent magnet synchronous generator, Maximum power control, Lyapunov methodology.

Resumen. En este artículo un esquema de control adaptable neuronal recurrente es aplicado a una turbina de viento con un generador síncrono de imán permanente. Debido al comportamiento variable de las corrientes de viento, la velocidad angular del generador es requerida a un valor específico para poder extraer la máxima potencia disponible. Para desarrollar la estructura de control, una red neuronal recurrente de alto orden es utilizada para modelar el sistema generador-turbina el cual es considerado desconocido; una ley de aprendizaje es obtenida utilizando el método de Lyapunov. Una ley de control, que estabiliza la dinámica del error de seguimiento de trayectoria es desarrollada utilizando Funciones de Control de Lyapunov. Mediante simulación, el esquema de control es aplicado a un punto de operación de máxima potencia en una turbina de viento de baja potencia.

Palabras clave: Redes neuronales, Turbina de viento, Generador síncrono de imán permanente, Control de máxima potencia, Método de Lyapunov.

1 Introduction

Renewable energies such as wind and solar energy conversion systems have driven attention during the past decade due to the environmental and economic concerns along with the reduction in the components cost. In remote areas such as rural populations are considered as sources that can replace conventional combustibles. Wind is a natural resource that features many advantages since it is clean and considerable reliable in some areas like the coast. In the wind energy conversion systems, the control problem consists on delivering the maximum power available from the wind to ensure the system reliability and security in order to deal with the variable nature of the generated energy. The crucial feature for wind energy generation systems is the instantaneous nature of electricity generation. The physical laws, which determine power delivery across a transmission grid, require a synchronized energy balance between power injection at generation points and power consumption at demand points plus transmission and distribution losses. Across the electric network, production and consumption are perfectly synchronized without any significant allowing for electricity storage. If generation and consumption get out of balance, even for a moment, both frequency and voltage will change with serious consequences for the power system and theirs users.

Since most of the research is actually driven to control large scale wind systems, most of the conversion topologies are based on doubly fed inductions generators. This paper focuses on controlling small wind turbines, which have a different impact area such as isolated communities and small scale applications. Wind turbines that operate at 2 to 10 kW output, generally use a permanent magnet synchronous generator (PMSG) which has a simple structure and reliable performance. The generator is the most important component in the generation system which also includes the wind turbine and the battery storage or grid connection.

Since the seminal paper [9], there has been continually increasing interest in applying Artificial Neural Networks (ANN) to identification and control since they are excellent approximators for nonlinear and stochastic models and have been implemented in several practical applications that deal with unknown dynamic systems. Lately, the use of recurrent neural networks is being developed, which allows more efficient modeling of the underlying dynamic systems [10] Three representative books [11], [14] and [15] have reviewed the application of recurrent neural networks for nonlinear system identification and control. In particular, [15] discrete time recurrent neural networks are applied to electrical generators, while [14] analyzes adaptive identification and control by means of on-line learning, where stability of the closed-loop system is established based on the Lyapunov function method. In [14], the trajectory tracking problem is reduced to a linear model following problem, with application to DC electric motors. In [11], analysis of Recurrent Neural Networks for identification, estimation and control are developed, with applications on chaos control, robotics and chemical processes. Recently, ANN have been successfully applied in identification and control of mechanical systems [1]. For wind generation systems, ANN have been considered as a convenient analysis tool for wind forecasting due to the simplicity of the model and the accuracy of the results [17]. For control applications, in [18] an ANN based wind velocity estimation and maximum power extraction control for small wind turbine generation system is developed using static networks. In [Chedid et al., 1999], a Wind Energy Generation System is analyzed using conventional and intelligent control approaches where an Neuro-Fuzzy scheme showed robustness and superior performance compared with the traditional control methods.

Many control applications deal with nonlinear processes in presence of uncertainties and disturbances. These phenomena must be considered for controller design in order to obtain the desired closed loop performance. In this article we use Recurrent High Order Neural Networks (RHONN) for applications to wind energy conversion systems, where we consider the presence of uncertainties and unmodeled dynamics. We develop an adaptive control scheme, which is composed of a recurrent neural identifier and a controller, where the former is used to build an on-line model for the unknown plant, and the latter to force the unknown plant to track the reference trajectory. An update law for the RHONN weights is proposed via the Lyapunov methodology. The control law is synthesized using the Lyapunov methodology. The proposed control scheme is displayed in Fig. 1. The algorithm is tested, via simulations, to control a 1 kW wind turbine for maximum power operating point. The simulation results verify that the neural controller can successfully satisfy the power demand.

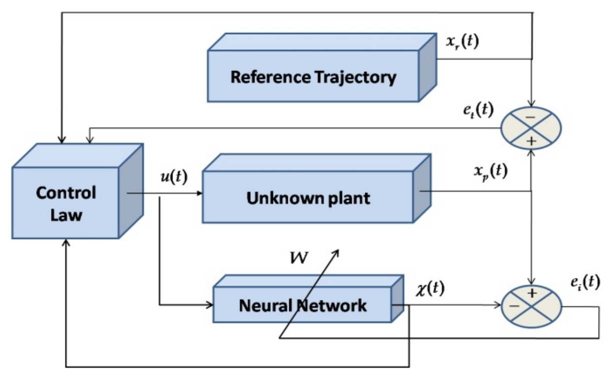

Fig. 1. Recurrent neural control scheme

2 System Model Description

In this work we focus on directly coupled synchronous generators. The wind turbine obtains power from wind currents and converts it into mechanical energy leading the shaft rotation. This system is displayed in Fig. 2. The obtained energy is proportional to the sweep area, the air density, the wind speed and the power coefficient as

$$P_m = 0.5\rho\pi R^2 V_w^3 C_p(\theta,\lambda) \quad (1)$$

where ρ is the air density, R is the turbine radius, $V\omega$ the wind speed, and $C_p(\theta,\lambda)$ is the coefficient of power conversion efficiency which depends on the blade pitch angle θ and the tip speed ratio λ The tip speed ratio is defined as

$$\lambda = \frac{R\omega_m}{V_\omega}$$

where ω_m is the rotor speed. The relationship of C_p and λ can be generated by experimentation. A typical curve is displayed in Fig. 3. As can be seen, for each wind speed, the maximum power available corresponds to one value of the turbine rotor speed. Then, by using a variable speed control scheme, the generator can operate at the maximum power.

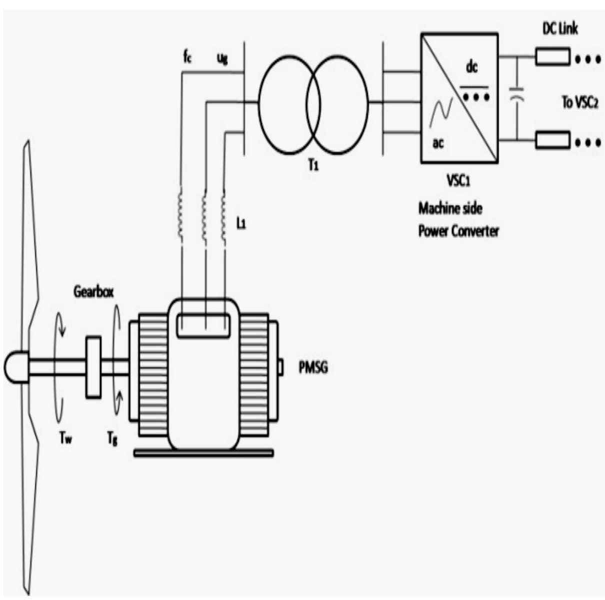

Fig. 2. Composition of a wind turbine **system**

C_p can be determined with the following relationship,

$$C_p = 0.22\left(\frac{116}{\beta} - 0.4\theta - 5\right)e^{-\frac{12.5}{\beta}} \tag{2}$$

where β is obtained from

$$\beta = \frac{1}{\frac{1}{\lambda + 0.08\theta} - \frac{0.035}{\theta^3 + 1}} \tag{3}$$

The aerodynamic power extracted from the wind is related with the torque by $P\omega = T\omega\omega_m$, then

$$T_\omega = 0.5\frac{\rho\pi R^2 V_\omega^3 C_p(\theta,\lambda)}{\omega_m} \tag{4}$$

$$T_\omega = 0.5\rho\pi R^3 V_\omega^2 \frac{C_p(\theta,\lambda)}{\lambda} \tag{5}$$

The generator in small wind turbines is typically a Permanent Magnet Synchronous Generator (PMSG), which is modeled by the following dynamic system

$$\frac{d\omega_m}{dt} = \frac{1}{J_a}\left(T_{\omega-g} - T_e - B_m\omega_m\right) \tag{6}$$

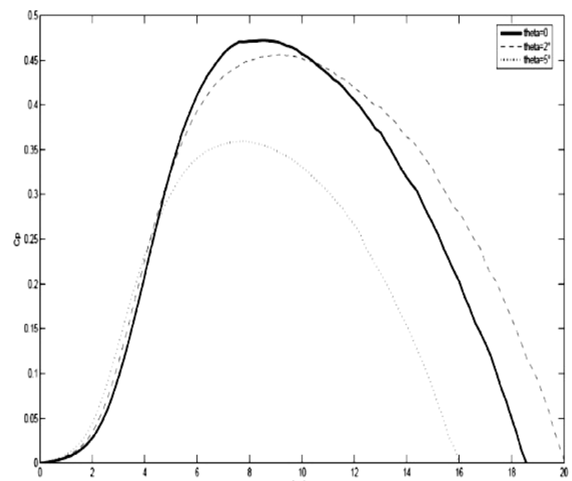

Fig. 3. Power Coefficient versus Tip Speed Ratio

where J_{eq} is the rotational inertia of the generator, B_m is the rotational damping, T_e is the electromagnetic torque and $T_{\omega\text{-}g}$ is the aerodynamic torque transferred from the wind.

For medium and small scale wind turbines, the variable speed wind turbine with multipole permanent magnet synchronous generator (PMSG) and full-scale power converter is frequently used. This synchronous generator connected to a power converter can operate at low speeds and does not require a gear transmission and a DC excitation system which gives the advantage of the high efficiently where its performance highly depends on how it is controlled; the control scheme depends on the variation of the wind speed which results on the change of the PMSG parametric data. The main disadvantage of this construction is the high cost of the permanent magnet and the fixed excitation of the field.

The PMSG is commonly modeled in the rotor reference frame applying the Park's transformation [Valenciaga et al., 2000]. The terminal voltage of the PMSG is defined by

$$[V_{gabc}] = -[R_{gabc}][i_{gabc}] + \frac{d}{dt}[\lambda_{gabc}] \tag{7}$$

$$V_q = -\left(R_g + \frac{d}{dt}L_q\right) i_q - \omega_g L_d i_d + \omega_r \Psi \tag{8}$$

$$V_d = -\left(R_g + \frac{d}{dt}L_d\right) i_d + \omega_g L_q i_q \tag{9}$$

where

R_g	Stator phase winding resistance (Ω)
L_q, L_d	Stator inductances in the quadrature axis (henry)
ω_g	Angular velocity of the generator (rad/s)
Ψ	Magnetic flux linkage (webers).

The dynamic model of the PMSG is derived in the two phase synchronous reference frames where the *q* axis is 90° after *d* with respect to rotating frame. The synchronization between the rotating frame *dq* and the three phase reference frame *abc* is hold by a phase link (PLL). The electromagnetic torque is expressed by

$$T_e = \frac{3}{2}P\left(\left(L_d - L_q\right)i_q i_d + \Psi_m i_q\right) \tag{10}$$

where *P* is the number of pole pairs in the generator.

The relation between the generator angular speed and the mechanical angular velocity ω_m is defined by $\omega_r = P_{\omega m}$. In general, $L_d = L_q = L$, then

$$T_e = \frac{3}{2}P(\Psi_m i_q) \tag{11}$$

And the complete model of the Wind Turbine with PMSG is given by

$$\frac{d\omega_m}{dt} = \frac{1}{J_a}\left(T_\omega - \frac{3}{2}P\Psi_m i_q - B_m\omega_m\right) \tag{12}$$

$$\frac{d}{dt}i_q = \frac{R_g}{L}i_q + \omega_g i_d - \frac{1}{L}\omega_r\Psi + \frac{1}{L}V_q \tag{13}$$

$$\frac{d}{dt}i_d = \frac{R_g}{L}i_q - \omega_g i_q + \frac{1}{L}V_d \tag{14}$$

The real and reactive power can be obtained from

$$P_s = V_d i_d + V_q i_q$$
$$Q_s = V_d i_q - V_q i_d$$

Different control strategies are usually applied to the machine-side converter as maximum torque control, unity power factor control, and constant stator voltage control. In general, the *d* axis of the reference frame is aligned along the permanent magnet flux position [Li and Chen, 2008]. In maximum torque control, the stator current is controlled to have the *q-component only,* $i_d=0$. Therefore, the generator provides the maximum possible torque without controlling the reactive power.

The control problem is established as follows: for a given wind speed we obtain the rotor angular speed that renders the maximum power coefficient at an optimal tip speed ratio. Then, the control algorithm will regulate the load given by V_d, V_q in order to maintain a desired output.

3 Recurrent Higher-Order Neural Networks

Artificial neural networks have become an useful tool for control engineering thanks to their applicability on modeling, state estimation and control of complex dynamic systems. Using neural networks, control algorithms can be developed to be robust to uncertainties and modeling errors.

Neural Networks consist of a number of interconnected processing elements or neurons. The way in which the neurons are interconnected determines its structure.

Recurrent networks. In a recurrent neural network, the outputs of the neuron are fed back to the same neuron or neurons in the preceding layers. Signals are transmitted in forward and backward directions. Artificial Recurrent Neural Networks are mostly based on the Hopfield model [3]. These networks are considered as good candidates for nonlinear systems applications which deal with uncertainties and are attractive due to their easy implementation, relatively simple structure, robustness and the capacity to adjust their parameters on line.

In [7], Recurrent Higher-Order Neural Networks (RHONN) are defined as

$$\dot{\chi}_i = -a_i\chi_i + \sum_{k=1}^{L} w_{ik}\prod_{j\in I_k} y_j^{d_j(k)}, \qquad i = 1,\cdots,n \tag{15}$$

where x_i is the th neuron state, L is the number of higher-order connections, $\{I_1, I_2, \ldots, I_L\}$ is a collection of non-ordered subsets of $\{1, 2, \ldots, m+n\}$, $a_i > 0$. w_{ik} are the adjustable weights of the neural network, $d_j(k)$ are nonnegative integers, and is a vector defined by $y = [y_1, \ldots, y_n, y_{n+1}, \cdots y_{n+m}]^T = [S(x_1), \ldots, S(x_n), S(u_1), \ldots, S(u_m)]^T$ with $u = [u_1, u_2, \cdots, u_m]^T$ being the input to the neural network, and $S(\cdot)$ a smooth sigmoid function formulated by $S(\chi) = \frac{1}{1+\exp(-\tau\chi)} + \zeta$. For the sigmoid function, τ is a positive constant and ζ is a small positive real number. Hence, $S(\chi)\in[\zeta,\zeta+1]$. As can be seen, (15) allows the inclusion of higher-order terms. By defining

$$z(\chi,u) = [z_1(\chi,u),\ldots,z_L(\chi,u)]\left[\prod_{j\in I_1} y_j^{d_j(1)},\ldots\prod_{j\in I_L} y_j^{d_j(L)}\right]$$

can be rewritten as

$$\dot{\chi}_i = -a_i\chi_i + \omega_I z(\chi,u) \quad i = 1,\ldots n \tag{16}$$

where $\omega_i = [\omega_{i,1},\ldots\omega_{i,L}]^\top$.

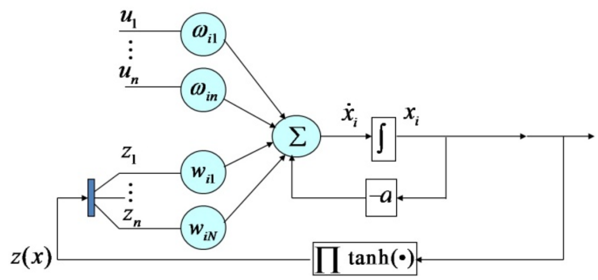

Fig. 4. Recurrent High Order Neural Network

In this paper,

This means that the same number of inputs and states is used. We also assume that the RHONN is affine in the control, so that (16) can be rewritten as

$$\dot{\chi}_i = -a_i\chi_i + \omega_i^T z(\chi) + \omega_{gi}u_i \quad i = 1,\ldots n \tag{17}$$

Reformulating (16) in a matrix form yields

$$\dot{x}_i = Ax + Wz(x) + W_g u \tag{18}$$

where $x\in\Re^n$, $W\in R^{n\times L}$, $z(x)\in\Re^L$, $u\in R^n$, and $A\in\Re^{n\times n}$. This RHONN structure is shown in Fig. 4.

For nonlinear identification applications, the term y_j in (15) can be either an external input or the identifier state of a neuron passed through the sigmoid function. Depending on the sigmoid function input, the RHONN can be classified as a Series-Parallel structure if $z(\cdot) = z(v)$, where v is an external input, or a Parallel one if $z(\cdot) = z(x)$, where x is the neural network state [14]. This terminology is standard in adaptive identification and control [4], [9]. The presented results can be extended to nonlinear systems with less inputs than states for the output tracking problem, where the full state measurement is not required, if neural observers are implemented [12].

4 Adaptive Recurrent Neural Control Scheme

In this work a RHONN is applied in a direct control scheme as can be seen in Fig. 1. The RHONN is used as an identifier for the unknown model, but the neural network weights will be adjusted in function of the tracking error in order to develop a control law based on a known structure but with adapting weights. This scheme is selected due to its easy implementation. Indirect control can be implemented using a similar algorithm by first doing online identification and then applying the control law [13]. For control applications, the RHONN features several advantages: the network architecture incorporates the nonlinear dynamics and having a more complex model compared with (15) due to the high order terms captures important characteristics of the nonlinear system to identify [14]. The stability and convergence properties of the RHONN as adequate models for nonlinear dynamic systems is further discussed in [7].

The nonlinear system (Wind turbine - PMSG) model can be described as

$$\dot{x}_p = f_p(x_p) + g_p(x_p)u \tag{19}$$

We propose to model the unknown nonlinear plant by the recurrent neural network

$$\dot{x}_p = \dot{\chi} + \omega_{per} = A\chi + W^* z(\chi) + \omega_{per} + W_g^* u \tag{20}$$

where $A = -aI$, $a \in \Re^+$, $x_p \in \Re^n$, $\chi \in \Re^n$, $z(\chi) \in \Re^L$, $W^* \in \Re^{n\times L}$, $W_g^* \in \Re^{n\times m}$, $u \in \Re^m$ and w_{per} represents the modeling error, with W^*, W_g^* being the unknown values of the neural network weights which minimize the modeling error.

In order to derive the learning laws and stability analysis, based on the Lyapunov approach, we state the next assumption:

Assumption 1. There exist unknown but constant optimal weights W^* such that the plant is described by the neural network plus a minimum bounded modeling error term ω^*_{per}. Then, the state x_p of the unknown dynamic system (20) satisfies

$$\dot{\chi}_p = Ax_p + W^* z(x_p) + \omega^*_{per} + sat\,(u) \tag{21}$$

$$\|\omega^*_{per}\| \le \omega^*_b \in \Re^+ \tag{22}$$

where all the elements are as defined earlier.

Remark 1. The weight matrices W^* is assumed to be unknown since ii is the optimal set which renders the minimum modelling error, defined as ω^*_{per}. Due to this fact, we use $W,$ as the approximation of the weight matrices W^* and ω^*_{per}, the modelling error, corresponds to $W^* \neq W$

Assumption 2. The trajectories of x_p are continuous and bounded for all $t > 0$.

We will design a robust controller which enforces asymptotic stability of the tracking error between the plant and the reference signal $\dot{x}_r = f_r\,(x_r, u_r)$ as

$$e\ := x_p - x_r \tag{23}$$

Its time derivative is

$$\dot{e} = A\chi + W^* z(\chi) + \omega^*_{per} + W_g^* u - f_r(x_r, u_r) \tag{24}$$

Now, we proceed to add and subtract the terms $\widehat{W}\ \Gamma z(x_r), Ae, \widehat{W}_g u$ so that

$$\dot{e} = Ae + W^* z(\chi) - \widehat{W}_Z(x_r) + w^*_{per} + \big(W_g^* - \widehat{W}_g\big)u + \big(-f_r(x_r, u) + Ax_r + \widehat{W} z(x_r) + W_g u\big) + A\big(\chi - x_p\big) \tag{25}$$

where $\widehat{W}, \widehat{W}_g$ are the estimated value for the unknown weight matrices W^*, W_g^*.

Let us assume that there exists a function $\alpha_r(t, \widehat{W}, \widehat{W}_g)$ such that

$$\alpha_r\big(t, \widehat{W}\big) = (\widehat{W}_g)^{-1}\big(f_r(x_r, u) - Ax_r - \widehat{W} z(x_r) - (x_r - x_p)\big) \tag{26}$$

Then, adding and subtracting to 25) the term $\widehat{W}g\alpha_r(t, \widehat{W}, \widehat{W}g\ )$ and simplifying we obtain

$$\dot{e} = Ae + W^* z(\chi) - \widehat{W} z(x_r) + \omega^*_{per} + \big(W_g^* - \widehat{W}_g\big)u - \widehat{W}g\alpha_r(t, \widehat{W}, \widehat{W}g\ ) + A\big(\chi - x_p\big) \tag{27}$$

Next, let us define $\widetilde{W} = W^*\text{-}\widehat{W}\ , \widetilde{W}_g = W_g^* - \widehat{W}_g$,

$\tilde{u} = u - \alpha_r(t, W)$ so that (27) is reduced to

$$\dot{e} = Ae + \widetilde{W} z(\chi) + W\big(z(\chi) - z(x_r)\big) + \omega^*_{per} + \widetilde{W}_g u + W_g\tilde{u} + A\big(\chi - x_p\big) \tag{28}$$

and by defining $\tilde{u} = u_1 + u_2$ with

$$u_1 = (\widehat{W}_g)^{-1}\Big(-\widehat{W}\,\Big(z(\chi) - z\big(x_p\big)\Big) - A\big(\chi - x_p\big)\Big) \tag{29}$$

equation (28) reduces to

$$\dot{e} = Ae + \widetilde{W}z(\chi) + \widehat{W}\left(z(x_p) - z(x_r)\right) + \omega_{per}^* + \widetilde{W}_g u + \widehat{W}g u_2 \quad (30)$$

Therefore, the tracking problem reduces to a stabilization problem for the error dynamics (30).

A. Tracking Error Stabilization

In order to perform the stability analysis for the system, the following Lyapunov function is formulated

$$V = \frac{1}{2}\|e\|^2 + \frac{\Gamma^{-1}}{2} tr\{\widetilde{W}^T\widetilde{W}\} + \frac{\Gamma_g^{-1}}{2} tr\{\widetilde{W}_g^T\widetilde{W}_g\} \quad (31)$$

$$\Gamma = diag\{\gamma_1, \ldots, \gamma_n\}, \quad \Gamma_g = diag\{\gamma_{g1}, \ldots, \gamma_{gn}\}$$

Its time derivative, along the trajectories of (30), is

$$\dot{V} = -a\|e\|^2 + e^T\widetilde{W}z(\chi) + e^T\widehat{W}\left(z(x_p) - z(x_r)\right) + e^T\omega_{per}^* + e^T\widetilde{W}_g u + e^T\widehat{W}_g u_2 + \Gamma^{-1}tr\left\{\dot{\widetilde{W}}^T\widetilde{W}\right\} + \Gamma_g^{-1}tr\left\{\dot{\widetilde{W}}_g^T\widetilde{W}_g\right\} \quad (32)$$

Replacing the learning laws

$$tr\left\{\dot{\widetilde{W}}^T\widetilde{W}\right\} = -\Gamma e^T\widetilde{W}z(\chi) \quad (33)$$
$$\dot{\widehat{\omega}}_{ij} = -\gamma_i e z(x_j)$$

$$tr\left\{\dot{\widetilde{W}}_g^T\widetilde{W}_g\right\} = -\Gamma_g\, e^T\widetilde{W}_g u \quad (34)$$
$$\dot{\widehat{\omega}}_{gij} = -\gamma_{gi}e_i u_j$$

In (32) we obtain

$$\dot{V} = -a\|e\|^2 + e^T\widehat{W}\phi_z(e, x_r) + e^T\omega_{per}^* + e^T\widehat{W}_g u_2 \quad (35)$$
$$\phi_z(e, x_r) = z(x_p) - z(x_r) = z(e + x_r) - z(x_r)$$

Next, we consider the following inequality [10],

$$X^TY + Y^TX \leq X^T\Lambda X + Y^T\Lambda^{-1}Y \quad (36)$$

which holds for all matrices $X, Y \in \Re^{nxk}$ and $\Lambda \in \Re^{nxn}$ with $\Lambda = \Lambda^T > 0$. Applying (36) to $e^T\widehat{W}\phi\ (e, x_r)$ with Λ =I, we obtain

$$\dot{V} \leq -a\|e\|^2 + \frac{1}{2}e^Te + \frac{1}{2}\|\widehat{W}\|\text{^}2\|\phi_z(e, x_r)\|^2 + e^T\omega\_per\text{^}* + e^T\widehat{W}_g u_2 \quad (37)$$

where $\|\widehat{W}\|$, is any matrix norm for $\widehat{W}$.

Since $\varphi_z(e,x_r)$ is Lipschitz with respect to e, then, there exists a positive constant $L\varphi$ such that $\varphi_z(e,x_r)^T \leq L\varphi\|e\|$. Hence (37) can be rewritten as

$$\dot{V} = -a\|e\|^2 + \frac{1}{2}\left(1 + L_\phi^2\|\widehat{W}\|^2\right)\|e\|^2 + e^T\omega_{per}^* + e^T\widehat{W}_{g_2^u} \quad (38)$$

To this end, we define the following control law:

$$u_2 = -(\widehat{W}_g)^{-1}\mu\left(1 + L_{\phi_z}^2\|\widehat{W}\|^2\right)e \quad \mu = diag\{\mu_1, \ldots, \mu_n\}, \quad \mu_i > \frac{1}{2} \quad (39)$$

which renders

$$\dot{V} \leq -a\|e\|^2 - \left(1 + L_\phi^2\|W^* - \widetilde{W}\|^2\right) \sum_{i=1}^{n}\left(\mu_i - \frac{1}{2}\right)e_i^2 + e^T\omega^*per \quad (40)$$

Considering that the modeling error is bounded by above by $\|\omega_{per}^*\| \leq \omega_b^*$,

$$\dot{V} \leq -a\|e\|^2 - \left(1 + L_\phi^2\|W^* - \widetilde{W}\|^2\right)\sum_{i=1}^{n}\left(\mu_i - \frac{1}{2}\right)e_i^2 + \|e^T\|\omega_b^*$$

From Corollary 5.2 from [5], there exists a class K_∞ function $\alpha_e(\|e\|)$, such that

$$\alpha_e(\|e\|) = a\|e\|^2 + \left(1 + L_\phi^2\|W^* - \widetilde{W}\|^2\right)\sum_{i=1}^{n}\left(\mu_i - \frac{1}{2}\right)e_i^2$$

then

$$\dot{V} \leq -\alpha_e(\|e\|) + \|e^T\|\omega_b^*$$

Outside the ball of radius $\alpha^{-1}(\omega_b^{*})$, we have that $e \to 0$ when $t \to \infty$ and from (33) $\widehat{\omega}_{ij}(t) \to 0$ then

$$\lim_{t\to\infty}\widehat{W} \to \widehat{W}_\infty \; and \; \lim_{t\to\infty}\dot{W} \to \dot{W}_\infty$$

and e and $\widehat{W}$ and uniformly ultimately bounded in

$$\{(e,\widehat{W}): \alpha(\|e\|) > \omega_b^*\}.$$

Now, let us consider the following lemm

Lemma 1 [4]. For scalar valued functions,

i) A function $f(t)$ which is bounded by below and not increasing has a limit when $t\mapsto\infty$.
ii) Consider the non negative scalar functions $f(t)$, $g(t)$ defined for all $t \geq 0$. If $f(t) \leq g(t)$, $\forall t \geq 0$ and $g(t) \in Lp$ then $f(t) \in Lp$ for all $p \in [1,\infty]$.

If $e = 0$, and $\widehat{W} \neq 0$, our tracking goal is achieved. Then, we proceed to prove the boundedness of the on-line weights. Since $\dot{V}$ is a negative semidefined function, not increasing and bounded by below, from Lemma 1 we have $\lim_{t\to\infty} V \to V_\infty$. Hence, V_∞ exists and it is bounded, then we have $\lim_{t\to\infty}\widehat{W} \to \widehat{W}_\infty$

Hence $\widehat{W}_\infty$ exists and it is bounded

From (40), that for all $e, W \neq 0$,

$$\lim_{t\to\infty} e(t) = 0 \tag{41}$$

Then, the control law to apply to the nonlinear system is defined by

$$u = \alpha_r x_r + u_1 + u_2 \tag{42}$$

$$u = (\widehat{W}_g)^{-1}\Big(f_r(x_r,u_r) - Ax_r - \widehat{W}z(x_r) - (x_r - x_p) - \widehat{W}\big(z(\chi) - z(x_p)\big) - A(\chi - x_p) - \mu\big(1 + L_\emptyset^2\|\widehat{W}\|^2\big)e\Big)$$

where $\alpha_r(x_r)$, u_1, u_2 are defined in equations (26), (29) and (39). This control law guarantees asymptotic stability of the error dynamics and therefore ensures the tracking of the reference signal.

B Simulation results

To evaluate the control capability of the RHONN controller, we now apply the developed approach on a small wind energy conversion system. The objective is to maximize the power extracted from the wind by controlling the rotor speed of the wind turbine. The states to control in the PMSG are i_d and ω_m. The current i_q will be driven to zero in order to minimize losses in the generator. The angular speed ω_m will be regulated at the optimum value which is obtained by measuring the wind speed and fixing the optimal value λ=7. The maximum power coefficient of this wind turbine is approximately C_p=0.42. The control signal applied directly to the machine-side converter is a three-phase sinusoidal voltage having the frequency of a PMSG. The control inputs are the load voltages in the $q-d$ reference frame. The parameters of the wind turbine are the following

R=1.525 m	L=0.00585 H
ρ=1.25 kg/m³	R=0.1 Ω
J=0.01 kg·m²	P=8
Ψ=0.175 Wb	

The approach is based on building a recurrent neural network identifier which obtains a reduced nonlinear model for the dynamics of i_d and ω_m The model is described by the following RHONN

$$\dot{\chi}_1 = -a_1\chi_1 + W_{1*}z(\chi_1) + V_d \qquad \dot{\chi}_2 = -a_2\chi_2 + W_{2*}z(\chi_2) + V_q \tag{43}$$

or in matrix form

$$\dot{\chi} = -a\chi + \widehat{W}z(\chi) + u \tag{44}$$

where $a_i > 0; W \in \Re^{2x6}, \chi = [i_d, \omega_m]^{\mathrm{T}}$ and

$$[z(\chi_j)]_i = \big(tanh(k\chi_j)\big)^i.$$

where we consider six high order terms.

For the speed control, we consider the simplified RHONN given by (43), and we select

$$a = diag\{17.5, 22.5\}, \Gamma = diag\{0.14, 0.10\}$$

$$k_1 = 0.085 \; k_2 = 0.008$$

Remark 2: The design terms can be selected by experimentation. In particular, large values of a_i relative to the maximum value of $W_{ij\infty}$ can derive in large oscillations. The selection of k_1 and k_2 is related with the effectiveness of the adaptation law, large values can saturate the sigmoid and produce large oscillation on the weight values. Furthermore, the learning rate values are related directly with the control law. If a large value is selected, a fast convergence to the minimum error can be achieved but at the cost of a large control effort.

For the control law (42), we choose μ=*10.* The simulation results are displayed in Fig. 5 to Fig. 8. The wind speed profile is displayed in Fig. 5 and represents the erratic nature of the input to the system. As can be seen in Fig. 7, the neural control achieves the desired performance with a tracking error not greater than 1%. This remaining tracking error is due to the number of high order terms and can be reduced by including more terms in the vector $z(\cdot)$. In Fig. 9-10 the time evolution of the neural network weights is displayed; the neural control algorithm ensures the bounded tracking error without requiring the convergence of these weights. The $d-q$ axis voltage components are displayed in Fig. 11.

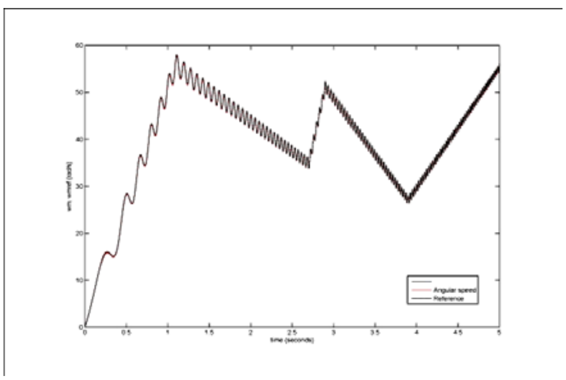

Fig. 5. Wind speed model

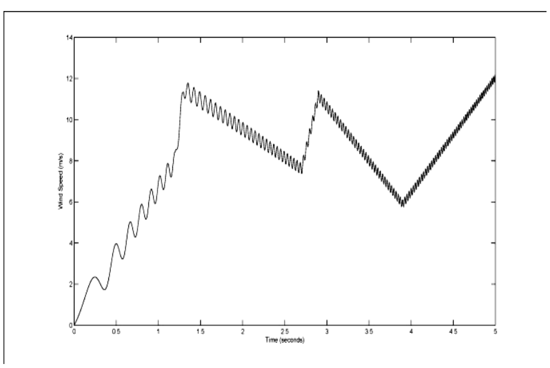

Fig. 6. Time evolution for the rotor angular speed

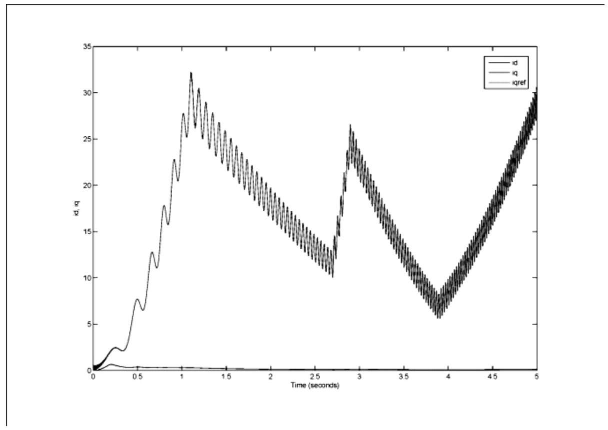

Fig. 7. Time evolution for i_d and i_q

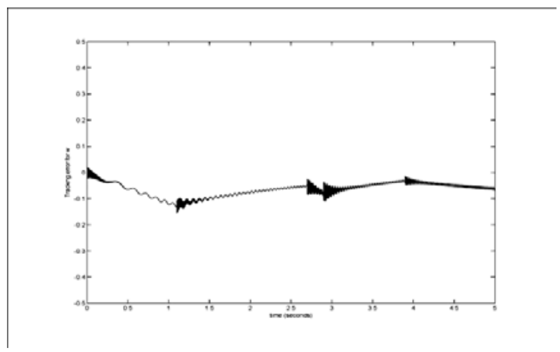

Fig. 8. Tracking error for the rotor angular speed

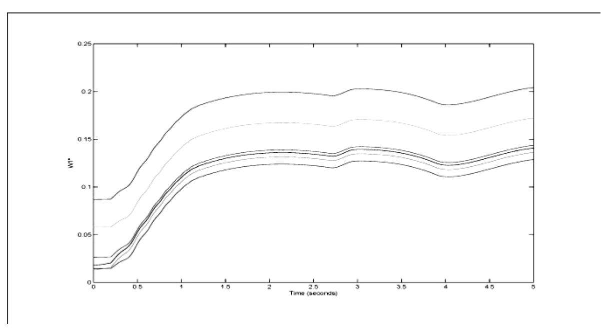

Fig. 9. Time evolution for neural network weigths W_1.

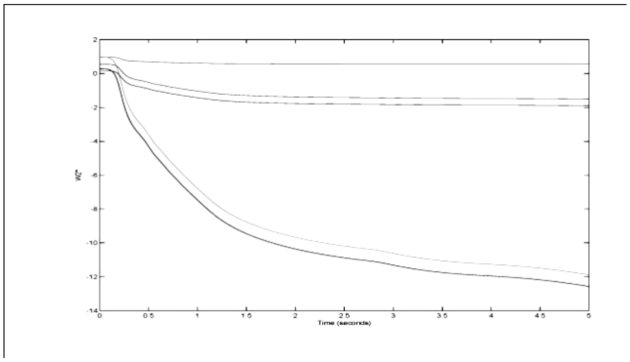

Fig. 10. Time evolution for neural network weigths W_{2*}

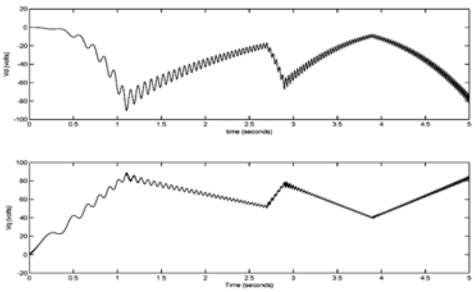

Fig. 11. Applied input

The neural control scheme features robustness to the uncertain nature of the wind speed profile where the angular speed required for maximum power tracking is accomplished even without knowing the wind turbine dynamic model; which is the main advantage of this work result in comparison with other nonlinear control schemes for maximum power tracking [22]. The implementation of high order neural networks in the controller is a novel result for wind energy generation systems since previous results have applied RNN only for prediction as in [20] where pitch angle is predicted, [2] where C_p curve is predicted, or [22] where the rotor speed is forecast from wind measurements but still required knowledge of the system model for control purposes.

7 Conclusions

In this paper an adaptive recurrent neural network controller is developed in order to implement a maximum power tracking scheme for a small wind turbine. The dynamical model of the wind turbine is presented and a High Order Neural Network is designed to model its dynamics. The control scheme is composed of a Recurrent Neural Network identifier that builds an on-line model for wind turbine and PMSG assumed to be unknown. A learning adaptation law is derived using the Lyapunov methodology. The proposed scheme is tested, via simulations, to control the angular speed of a 1 kW synchronous generator in the *d-q* reference frame in order to achieve maximum power tracking. Further work aims to implement this controller in real time laboratory experiments and integrating a battery bank to the system.

Acknowledgements.

The first author thanks PROMEP Project PROMEP/103.5/07/2595 for supporting this research. The second author thanks CONACyT, Mexico, Project FOMIX 66192, for supporting this research.

Referencias

1. **Baruch, I. & Olivares, J. L. (2005).** Implementacion de un multimodelo neuronal jerárquico para identificación y control de sistemas mecánicos, *Computación y Sistemas,* 9 (1), 28-40.
2. **Chedid, R., Mrad, F. & Basma, M. (1999).** Intelligent control of a class of wind energy conversion system, *IEEE Transactions on Energy Conversion,* 14 (4), 1597-1604.
3. **Hopfield, J. (1984).** Neurons with graded responses have collective computational properties like those of two state neurons, *Proceedings of the National Academy of Sciences*, 81 (10), 3088-3092.
4. **Ioannou, P. A. & Sun, J. (1996).** *Robust Adaptive Control,* Upper Saddle River, New Jersey: Prentice Hall.
5. **Khalil, H. (2002)** *Nonlinear Systems*. Upper Saddle River, New Jersey: Prentice Hall.
6. **Khalil, H. (1996).** Adaptive Output Feedback Control of Nonlinear Systems Represented by Input-Output Models, *IEEE Transactions on Automatic Control,* 41 (2), 177-188.
7. **Kosmatopoulos, E. B., Christodoulou, M. A. and Ioannou, P. A. (1997).** Dynamical neural networks that ensure exponential identification error convergence, *Neural Networks,* 10 (2), 299-314.
8. **Li, H., & Chen, Z. (2008).** Overview of different wind generator systems and their comparisons, *Renewable power generation*, 2 (2), 123 – 138.

9. **Narendra, K. S. & Parthasarathy, K. (1990).** Identification and control of dynamical systems using neural networks, *IEEE Transaction on Neural Networks,* 1(1), 4-27.
10. **Poznyak, A. S., Yu, W., Sanchez, E. N. & Perez, J. P. (1999).** Nonlinear adaptive trajectory tracking using dynamic neural networks, *IEEE Transaction on Neural Networks,* 10 (6), 1402-1411.
11. **Poznyak, A. S., Sanchez, E. N. & Yu, W. (2000).** *Differential Neural Networks for Robust Nonlinear Control*, Singapore: World Scientific.
12. **Ricalde, L. J. & Sanchez, E. N. (2005).** Inverse Optimal Nonlinear High Order Recurrent Neural Observer, *International Joint Conference on Neural Networks IJCNN*, Montreal, Canada, 361-365.
13. **Ricalde, L. J. & Sanchez, E. N. (2008).** Output tracking with constrained inputs via inverse optimal adaptive recurrent neural control, *Engineering Applications of Artificial Intelligence,* 21 (4), 591-603.
14. **Rovitahkis, G. A., & Christodoulou, M. A. (2000).** *Adaptive Control with Recurrent High-Order Neural Networks*. New York: Springer Verlag.
15. **Sanchez, E. N., Alanis, A. Y. & Loukianov, A. G. (2008).** *Discrete-Time High Order Neural Control Trained with Kalman Filtering*. Berlin: Springer Verlag.
16. **Sanchez, E. N. & Ricalde, L., (2003).** Chaos Control and Synchronization, with Input Saturation, via Recurrent Neural Networks, *Neural Networks,* 16 (5-6), 711-717.
17. **Senjyu T., Yona, A., Urasaki, N. & Funabashi, T. (2006).** Application of recurrent neural network to long-term-ahead generating power forecasting for wind speed generator, *Power Systems Conference and Exposition PSCE,* Atlanta, USA, 1260-1265.
18. **Shi, K. L., Li, H. (2004).** A novel control of a small wind turbine driven generator based on neural networks, *IEEE Power Engineering Society General Meeting*, Denver, USA, 1999 - 2005.
19. **Valenciaga, F., Puleston, P. F., Battaiotto, P. E. & Mantz, R. J. (2000).** Passivity/Sliding Mode Control of a Stand Alone Hybrid Generation System, *IEE Proceedings on Control Theory Applications,* 147 (6), 680-686.
20. **Yao, X., Su, X. & Tian, L. (2009).** Pitch angle control of variable pitch wind turbines based on neural network PID, *4th IEEE Conference on Industrial Electronics and Applications, ICIEA 2009*, Xi'an, China, 3235–3239.
21. **Yin, M., Li, G., Zhou, M. & Zhao C. (2007).** Modeling of the wind turbine with a permanent magnet synchronous generator for integration, *Power Engineering Society General Meeting*, Tampa, USA, 1-6.
22. **Zhang J., Cheng, M. & Chen, Z. (2007).** Nonlinear Control for Variable-Speed Wind Turbines with Permanent Magnet Generators, *International Conference on Electrical Machines and Systems*, Seoul Korea, 324-329.

Luis Ricalde Castellanos

Received the BSME from ITM, Yucatan, Mexico in 1999, the MSEE and PhD in Automatic Control from CINVESTAV-IPN, Guadalajara in 2001 and 2005. Since 2007, he has been with FI-UADY as Professor of Mechatronics Engineering. His research interest centers in neural network control, constrained inputs control and renewable energies.

Edgar N. Sánchez Camperos

Obtained the BSEE from Universidad Industrial de Santander in 1971, the MSEE from CINVESTAV-IPN, Mexico in 1974 and the Docteur Ingenieur degree from INP, Grenoble in 1980. His research interest centers in Neural Networks and Fuzzy Logic applied to Automatic Control. He is member of the SNI, level III and has published more than 100 technical papers and participates as Associate Editor for several journals.

Braulio José Cruz Jiménez

Recieved the BSEE from ITM, Yucatan, Mexico on the digital systems field. Received the MS on Automation from ITESM, Monterrey, Mexico. Since 2005 he works as full time professor for Mechatronics Engineering in UADY. His research field centers on Hybrid systems control, nonlinear control and biomedical signal processing.